Comparative Study of ZnS and FeS_2 Buffer Materials in CZTS Heterostructure Based Solar Cells.

I- Case FP-LAPW calculations

N. Ouarab[a, b,*], M. Boumaour[a] A. Haroun[b] and A. Bahfir[a, c]

[a)] - Semiconductor Technology Research Center for Energetic-(CRTSE), 02, Bd Frantz Fanon Algiers, Algeria.
[b)] - Quantum Physics and Dynamic Systems Laboratory, Ferhat Abbas University, Sétif 19000, Algeria.
[c)] - University of Sciences and Technology Houari Boumediene, Algiers, Algeria.
E-mail : ouarab_nourdine@yahoo.fr

Abstract

In actual thin film PV device based on chalcopyrite CIGS absorber, zinc blend ZnS has proven to replace successfully toxic and expensive CdS buffer layer, with high efficiency of about 18 %. In the other class of materials based on chalcogenide absorber where costly and scarce Indium and Gallium are replaced by Zinc and Tin, ZnS mix rather badly with CZTS due to small lattice misfit of 1.38% and large valence band offsets of 0.9 eV. Among possible alternatives to ZnS mixed with CZTS, the pyrite FeS_2 is a promising candidate who can address economic and environmentally issues. To do so, we investigate in a comparative study the structural, electronic and optical properties of ZnS and new introduced pyrite FeS_2 as a buffer layer in kesterite CZTS based solar cells. First-principles calculations are performed using FP-LAPW method implemented in Wien2k code within the framework of Perdew-Burke-Ernzerhof-GGA approximation. The addition of the Hubbard term U in LDA+U/ (GGA+U) approximation was necessary to correct the energy gaps. The calculated band structure gives reliable results close to the experimental values of 3.78 and 1.29 eV which are direct gaps located at Γ point in BZ for ZnS and CZTS, respectively. For FeS_2, the modified Becke-Johnson potential is used to calculate its band gap and it gives a value of 1.093 eV. It is found that FeS_2 can be used as an efficient buffer in CZTS heterostructure solar cells.

Keywords : CZTS solar cell, ZnS, FeS2, Optical properties, Surface and Interface.

1. Introduction

Solar cells based kesterite-Cu_2ZnSnS_4 showed recently an improved conversion efficiency of 11.1% [1] and appears as a promising candidate absorber for future thin film photovoltaic (PV) industry as compared to the best performing CuGaInS (CGIS) solar cells absorbers. The CZTS is a relatively new photovoltaic material constructs basis non-toxic, more abundant and less expensive chemical elements then is expected to be interesting for environmentally amenable solar cells [2-8]. This material has interesting optical and electronic properties; it has shown a direct band gap around 1.5 eV and an absorption coefficient of ~10^4 cm^{-1} in the visible range, which is ideal to achieve high solar-cell conversion efficiency [8]. It has been found in some theoretical and experimental studies that the Kesterite structure is the most stable among the Stannite and Wurtzite structure with the $I\bar{4}$ symmetry space group [7, 9, 10], contains as lattice parameters a_{czts} = 5.42 Å and c_{czts} = 10.90 Å, and it has a good lattice mismatch with ZnS ($F\bar{4}3m$) in the normal conditions which has as lattice parameter a_{ZnS} = 5.41 Å [11, 12]. Now, the interest of PV industry is to manufacture high efficiency solar cells with competitive and friendly-environmental materials and technologies. Thin film CdS/CIGS solar cells have shown to be reliable and has yielded high efficiency of about 18 % in similar devices made without CdS buffer layers [13]. One other issue is the cost and scarcity of Indium and Gallium especially for large scale productions. In recent novel thin film PV devices, both CIGS absorber and CdS buffer layer have been replaced by CZTS and ZnS, respectively. Tranposing the same configuration, it was found that ZnS mixes rather badly with CZTS due to some intrinsic fundamental inconsistency raisons. The large lattice mismatch and stress forces at interface can directly affect band offsets, optical properties and reduce interface potential which fosters electronic transport between the two materials. In the point of elastic stability view, ZnS have a small lattice mismatch with CZTS and hardly affects the chemical bonds at the interfaces and creates a potential gate for both electron and hole carriers. In the other case of ZnS/CZTS interface, the valence band offset is over 0.9 eV and the conduction band offset is over 1.3 eV [14, 15]. ZnS appears then as an inactive insulator phase with CZTS absorber [2]. Owing to this critical situation, the accurate crystallographic orientations have to be taken into account to expect promising results. Experimentally however, the fine control of crystalographic orientation is not easily feasible, other than by well-known but very expensive epitaxial techniques. One way would be to seek for a

specific material which possesses particular crystalline structure while preserving economic and environmental issues. A possible alternative can be FeS_2; this material shows interesting optical, electrical and transport properties [16,17] and we will investigate by numerical simulation the possibility of its insertion as a buffer layer on CZTS absorbent material .

In this paper, the first-principles calculation are performed by using the full-potential linear augmented plane waves plus local orbitals method (FP-LAPW) as implemented in Wien2k-package [18], with Perdew-Burke-Ernzerhof (PBE) exchange-correlation functional [19] as well as the LDA+U/GGA+U orbital potential approximation that is necessary to correct the energy gaps for semi-conductor materials [20]. We focus in particular on interfaces between CZTS relaxed structure and ZnS(001), ZnS(½[110]) and pyrite FeS_2(001) optimized volumes important for solar-cell applications. The band structure is calculated for each material in bulk. The band offset between these structures is quantitatively analyzed from each calculated band gap. We also discuss how these band offsets could affect optical properties, as absorption coefficient, optical conductivity and dielectric functional.

2. *Computational details*

The kesterite-CZTS is the most stable phase; its total energy is smaller than the wurtzite-stannite structures [21]. This is the reason why we will focus our study on the interaction with a zinc-blende structure. We however must take into account many structural considerations. It is well known in semiconductor materials that the structural properties significantly affect the electronic and optical properties [10]. In the first case, we use density functional theory (DFT) calculations to optimize structural parameters of bulk FeS2, ZnS and CZTS separately.

Calculations are performed as mentioned above, by using relativistic FP-LAPW+lo method applying the PBEsol-GGA exchange-correlation functional, because the errors percent of the surface exchange energy are 2.7% better than the standard PBE that equal to 11% [19]. Brillouin-zone integration was performed on Γ-centered symmetry reduced Monkhorst-Pack k-meshes [22]. Bulk phase calculations have been carried out using shifted k-special points of 4×4×4, 8×8×8 and 10×10×10 meshes for CZTS, ZnS and FeS_2 primitive unit cells, respectively. Also we use the value of 9, 8 and 8 of $R_{mt}K_{max}$ product parameter for same simple, respectively. This product parameter will determines matrix size to esteem time calculations and the convergence criterion is fixed to 10^{-4}. Where K_{max} is the plane wave cut-off and R_{mt} is the smallest of all atomic sphere radii. Bulk band gaps are treated by using LDA+U/GGA+U potential orbital to correct the energy gaps, and we chose the U value parameter to be adequate for band gaps observing in experimental studies. In the case of FeS_2, the modified Becke-Johnson potential is supported in Wien2k-package to calculate band gap and to see the role of hybrid HF/DFT method for FeS_2 structure. We also considered the B3LYP functional form (Becke's three-parameter hybrid exchange and Lee–Yang–Parr correlation functionals) [23]. The atomic positions are relaxed for CZTS structure to minimize stress and Hellmann-Feynman forces because we observed when we suppose Wyckoff position for Sulfur in CZTS and FeS_2 structures, the forces are large. The volume optimization of these structures is necessary to minimize total energy and to avoid the artifact structure when we construct a ZnS (001)/CZTS, ZnS(½[110])/CZTS and FeS_2 (001)/CZTS super-cells. The valence band offset ΔE_v (A/B) phases is calculated by the means of the core level energy [15], and is defined as:

$$\Delta E_v(A/B) = \Delta E_{b-v} + \Delta E_{I-v} \quad (1)$$

The bulk term $\Delta E_{b-v} = E_v^A - E_v^B$ is the difference of the maximum of valence band of each material. The term ΔE_{I-v} is the potential alignment at the interface directly calculated from band structure. As for conduction band offset ΔE_c is given by:

$$\Delta E_c(A/B) = \Delta E_v(A/B) + \Delta E_g(A/B) \quad (2)$$

And ΔE_g (*A/B*) is the difference of gap energy between A and B in heterostructure. For optical properties, the theoretical framework is based here on electric dipole hypothesis and quantum mechanics theory. The complex dielectric function describes the polarization response of the material to an externally applied electric field.

$$\zeta(\omega) = \zeta_1(\omega) + i\zeta_2(\omega) \quad (3)$$

The imaginary part of dielectric function is calculated from the joint DOS [24] from the following expression:

$$\zeta_2(\omega) = \frac{e^2 \mathrm{h}}{\pi m^2 \omega^2} \sum_{v,c} \int_{BZ} |Mme|^2 \, \delta(\omega_c - \omega_v - \omega) d^3k \quad (4)$$

$|Mme|^2$ is the momentum matrix elements for dielectric transitions between valence and conduction bands; δ is the Dirac's delta function which defines the electric field. The real part $\zeta_1(\omega)$ can be derived from the imaginary part by means of Kramers-Kronig transformations:

$$\zeta_1(\omega) = 1 + \frac{2}{\pi} P \int_0^\infty \frac{\omega' \zeta_2(\omega')}{\omega'^2 - \omega^2} d\omega' \quad (5)$$

P is the constant of the integral. And the absorption coefficient α (ω) is given by [25].

$$\alpha(\omega) = \frac{\sqrt{2}\omega}{c} \left[\sqrt{\zeta_1^2(\omega) + \zeta_2^2(\omega)} - \zeta_1(\omega) \right]^{1/2} \quad (6)$$

where c is the speed of light. The refractive index *n* (ω) is important for optical properties calculations and it is

expressed by real and imaginary parts of dielectric function as:

$$n(\omega) = \left[\frac{\zeta_1(\omega)}{2} + \frac{\sqrt{\zeta_1^{\,2}(\omega) + \zeta_2^{\,2}(\omega)}}{2} \right]^{1/2} \quad (7)$$

3. *Results and discussion*

3.1 Structural properties

A special attention has been given to the structural relaxation to draw the curve of total energy as function of cells volume as shown in Fig. 2, which can give an accurate prediction of the equilibrium volumes of these structures. A Birch-Murnaghan [26] equation of state is used to obtain the equilibrium volume (V_0), total energy (E) and lattice parameters (a, c and tetragonality ratio c/a). The results have been listed in Table 1.

From Table 1, the c/a ratio is very close to 2 for CZTS material. This is in accordance with most of recent experimental data [27-28]. We observe that ZnS is the binary cubic similarity for CZTS and we note that ZnS can grow normally on CZTS in equilibrium conditions. We are in particular interested on two crystallographic orientations as depicted in Fig. 1: The first, when ZnS is epitaxed at (001) direction from CZTS. Another, when the ZnS is epitaxed in the (½[110]) orientation for the reason to increase forces and stress, also to reduce the potential gate. For the first case, the conversion efficiency is in order of 3.08% of ZnS ultrathin layer of thickness of 5 nm. In the second one, the result show that the turned ZnS structure by 45° at the interface can contribute directly to band offset calculations and how the last can affect solar-cell conversion efficiency of our system. The method to grow ZnS layer at particular (½[110]) direction is unfortunatly not directy applicable. We noticed that this twisted ZnS structure by 45° have the same shape of the pyrite structure FeS_2 at the one difference of the number of sulfur atoms in each one and these Wyckoff positions (Fig.2 c).

On the other hand, the CZTS possesses five in-equivalent atoms located by Wyckoff positions as : {(0, 0, 0), (½, 0, ¼)}, (0, ½, ¼), (0, 0, ½), {(¼, ¾, 5/8), (¾, ¼, 5/8), (½, ½, 3/8), (¾, ¾, 3/8)} for Cu_2, Zn, Sn, and S4, respectively. This configuration shows that the Hellmann-Feynman forces are larges for Sulfur atoms, and then all lattice vectors and atomic positions were fully relaxed by minimizing the quantum mechanical stresses and forces. Eos fitting gives new lattice parameters for CZTS correspondingly to the smallest energy as a_{czts}= (5.452±0.002) Å, c_{czts} = (10.801±0.002) Å and c/a = (1.984±0.002). This result is in agreement with H. Nozaki et al which find the following lattice parameters a_{czts} = 5.438 Å, c_{czts} = 10.857 Å [29]. V. Kheraj shows that the lattice parameters calculated for the CZTS sample S4 from XRD analysis come out to be 5.427 Å and 10.854 Å for a and c, respectively [30]. As for ZnS, the volume optimization is insisted by Birch-Murnaghan equation of state giving a_{ZnS} = (5,378 ±0.002) Å were in good agreement to the theoretical studies and experimental observations [11, 31-33]. By the same way, we also calculate the lattice parameter of pyrite FeS_2 and found that a_{FeS2} = (5.3508±0.002) Å. The structural properties of bulk FeS_2 are calculated by the relationship between total energy and cell volume.

TABLE I. THEORETICALLY AND EXPERIMENTALLY CALCULATED LATTICE PARAMETERS OF ZINC-BLNEDE ZNS, PYRITE FES2 AND KESTERITE CZTS

	a (Å)	c (Å)	c/a	Reference
ZnS(001)	5.378	—	—	This work
	5.342			[11]
	5.335			[34]
	5.410			Exp[31]
FeS_2(001)	5.31	—	—	This work
	5.382			[24]
	5.266			[36]
	5.416			Exp[23]
CZTS(001)	5.452	10.801	1.984	This work
	5.427	10.854	2.000	[30]
	5.438	10.857	1.996	[29]
	5.424	10.861	2.002	Exp[27]

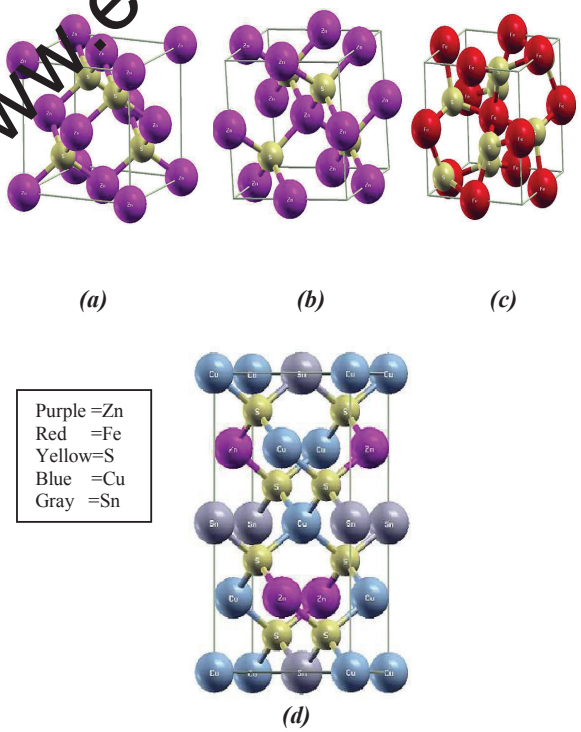

Figure 1. Crystalline structures of: *a)*-Zinc blend ZnS(001), *b)*-Zinc-blend ZnS(½[110]), *c)*- Pyrite FeS_2(001) and *d)*- Kesterite CZTS

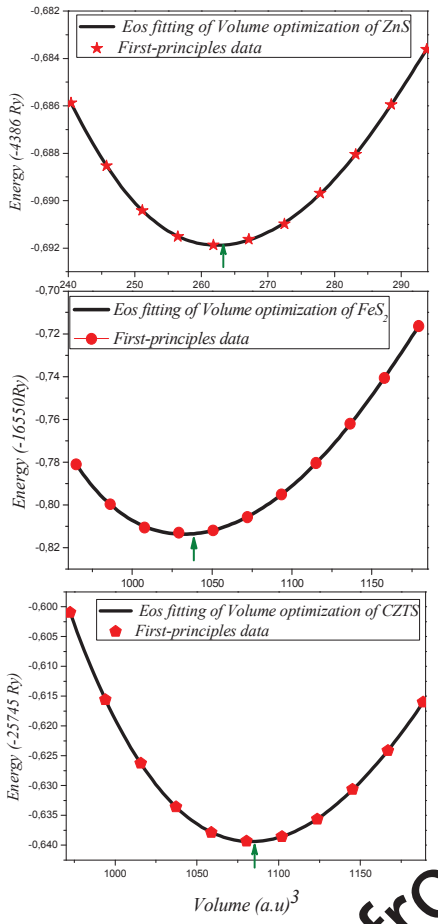

Figure 2. Eos fitting of the relationship between total energy and volumes of ZnS, FeS2 and CZTS. The green arrow shows the equilibrium volumes.

G. Qiu *et al* [24] used the CASTEP package (pseudo-potential- code) to calculate a total energy as a function of lattice parameter a_0 and of the Wyckoff parameter *u*. They found that 'a' value of lattice parameter of FeS_2 to be equal to 5.382 Å. This result is very close to our calculation and also to experimental value of 5.416 Å [23]. Joseph Muscat *et al* [36] computed the lattice parameter of the optimized structure of FeS_2 using HF, LDA,GGA and B3LYP treatments of exchange-correlation potential as implemented in Crystal 98 and CASTEP package and their result is ~ 5.299 - 5.414 Å.

3.2 Electronic properties

The calculated band gap energies is based on GGA+U approximation for CZTS and ZnS at equilibrium structure. "Fig. 3" shows the theoretical band gap of these structures. The Fermi level of each band structure is set to 0 eV. These calculations reveal a direct bandgap at the Γ point of the Brillouin zone for both ZnS and CZTS. For the analysis of the band structure of CZTS it is likely that the dispersion of the S p – Cu d anti-bonding states overlap to form at valence band, where the top of the valence band remains fairly unaltered. At the bottom of the valence band of both crystals ZnS and CZTS are mostly derived from S-3s states and slightly mixing to 3d Zn. This result is in agreement with some theoretical and experimental studies that show a band gap of ZnS around 2.16 - 3.8 eV [11, 35, 37]. For the case of CZTS, Dan Huang *et al* used in GGA+U approximation, effective values U parameters (5.2, 6.5, and 3.5 eV) for Cu3d, Zn3d and Sn4d states, respectively [38]. The band gap energy is given to be around 1.5 eV according to experimental studies of Cu-poor and Zn-rich CZTS samples [39-42]. In our study, we use the similar way in Wien2k package [18] and we take J = 0 for all states; then we use only U parameters for $Cu_2$3d and Zn3d states, with 5.02 and 5.42 eV values, respectively. The result gives a value of 1.29 eV for the direct gap located at Γ point in BZ. Next, the band structure calculated for ZnS using the values of U = 3.10 eV for Zinc and 1.40 eV for Sulphur gives a reliable band gap close to the experimental value [44], and Eg ≈ 3.62 eV which is a direct gap located at Γpoint in BZ. The choice of how to use U parameter in CZTS of what atoms

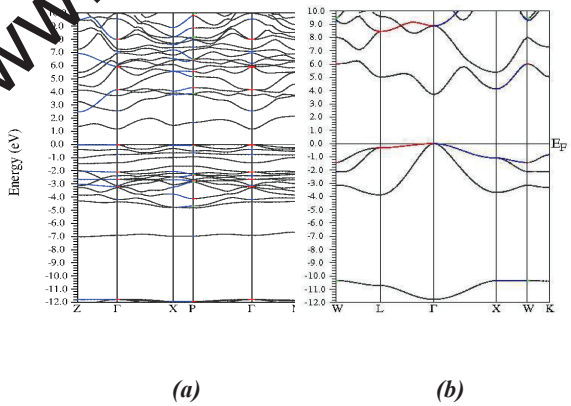

(a) *(b)*

Figure 3. The band structures calculated by means of LDA+U/GGA+U approximations of *(a)*- Kesterite CZTS and *(b)*- Zinc-blende ZnS which are Γ direct band gap of values of 1.29 and 3.62 eV, respectively.

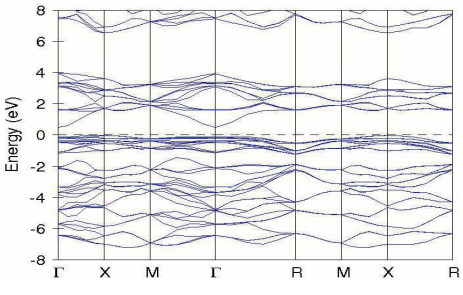

Figure 4. The band structure of Pyrite FeS_2 calculated by LMTO-code

is provided by calculating of electronic density at (111) direction. The result shows that there are two regions ; the strong and weak correlation zone. We used then only the U parameter for atoms located at strong correlation zone. For FeS_2, we use the modified Becke-Johnson potential to calculate its band gap and to see the role of hybrid HF/DFT method for the Pyrite structure. This method gives a value of 1.093 eV of band gap which is verry close to the experemental result. Also, we use the LMTO-code to draw the band structure using the case of non spin-polarized with combined corrections and we use the exchange-correlation of Perdew-Wang[43]. The result shows two natures of band gap : The first is an indirect band gap of 0.482 eV between points with coordinates (0.4, 0.0, 0.0) and (0.0, 0.0, 0.0) at the Brillouin zone. The second is a direct band gap of 0.593 eV at the point (0.4, 0.0, 0.0), (see "Fig. 4"). The phenomenology of valence and conduction band offsets between absorber and buffer materials is not easy for the conversion effeciency of solar cells[45]. Then, the large positive conduction band offset create a potential gate for both electron and hole carriers.

In this work, the relatively small negative conduction band offset of -0.19 eV at the CZTS/FeS_2 interface indicates that FeS_2 can be used as buffer layer for the CZTS solar cells. On the other hand, the large positive conduction band offset of 0.6 eV at the CZTS/ZnS interface causes an energy barrier for the electrons generated in the CZTS absorber and decreasing the conversion efficiency (see "Fig. 5"). Although, Calculations of lattice misfit of both materials and internal stress shows that the FeS_2 material have a good lattice mismatch of 1.89% in comparaison with ZnS near the interface with CZTS absorber. The valence and conduction band offsets of pyrite FeS_2 are smaller in relation to these of ZnS due to the strain induced by increased lattice misfit between CZTS and FeS_2 of about 1.89% in comparaison with lattice mismatch between CZTS and ZnS of about 1.37%. Then, the large lattice misfit can cause defect states in structural properties and dipole moment as well as the band offset can also be affected [42].

3.3 Optical properties

The study of optical properties is based here on complex dielectric function describing the linear response of these materials to externally applied electromagnetic waves. Since the imaginary part of dielectric function is related to joint DOS [24], interpretation and analysis of optical properties are based on projected density of states and electrical band structure. The optical properties as dielectric function, refractive index and absorption coefficient are calculated over a photon energy range extended to 10 eV. In figure 6, we present frequency dependent real and imaginary part of dielectric function of CZTS, ZnS and FeS_2 materials calculated using FP-LAPW method.

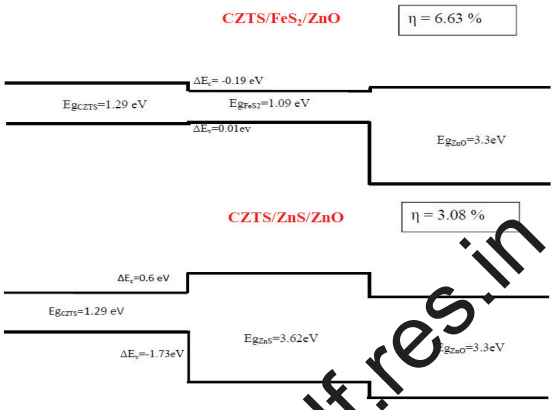

Figure 5. Band offsets quantitatively calculated for CZTS/FeS_2/ZnO and CZTS/ZnS/ZnO.

Furthermore, the imaginary part of dielectric function is written as function of the momentum matrix elements for dielectric transitions between valence and conduction bands, and then all critical peaks can find origins in inter-band transitions. The first analysis of imaginary part of dielectric function $\varepsilon_2(E)$ shows that there are five intense peaks (Fig. 6) marked as : A (4.29 eV) ,B (5.59 eV), C (6.84 eV), D (7.72eV) and E (8.26 eV) for ZnS and five other peaks as F (2.86 eV), G (3.34 eV), H (5.37 eV), I (7.38 eV) and J (9.41eV) for FeS_2 material. It is observed that the threshold

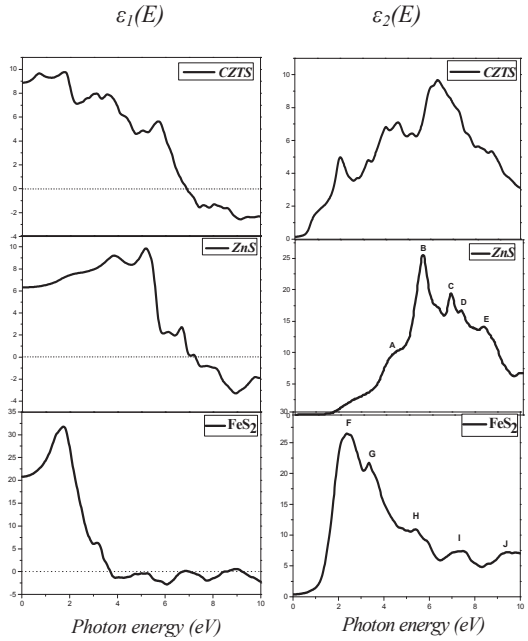

Figure 6. Real and imaginary part of dielectric function of Kesterite-CZTS, Zinc blende-ZnS and Pyrite FeS_2.

of absorption occurs at 3.58±0.02eV for ZnS material. This point represents splitting between Γ_{15v}-Γ_{1c} and gives the threshold of the direct electronic transitions band between the highest of the valence band and the lowest of the conduction band. Besides, the origin of these peaks is assigned to the inter-band transitions formed by the electronic transfer between the occupied states 4s or binding of Zn atom toward the vacant or anti-binding states 3p of Sulfur. For FeS_2, all the transitions are mainly between S-3p and Fe-3d states. All these transitions are originated at X direct bandgap and between Γ- X indirect bandgap in BZ. The threshold of absorption occurs at the energy (1.04± 0,02) eV for FeS_2 material which is approximately the value of bandgap. Our calculations show that ZnS and FeS_2 are optically isotropic contrary to CZTS material, then the average value of its dielectric function is calculated by the relationship : $\varepsilon_i(\omega) = \{2*\varepsilon_\perp+\varepsilon_\parallel\}/3$. The i index shows the real or the imaginary part of dielectric function and $\varepsilon_\perp$, $\varepsilon_\parallel$ are the components perpendicular and parallel to the z axis [22, 46]. The crystalline relaxation of CZTS proves that the positions of Sulfur are not those of Wyckoff. A direct consequence of this calculation shows that the CZTS is anisotropic. In the point of practice view, the dislocation affects directly the physical properties of the material and it has tendency to widen its domain. The threshold of absorption of CZTS occurs at the energy (1.26 ± 0, 02) eV; this point shows that the direct electronic transitions are created between the highest of the valence band and the lowest of the conduction band at Γ point in BZ. The critical peaks in $\varepsilon_2(\omega)$ spectrum are due to the electronic transitions from 3d-Zn state toward 3d-Cu state and from 3d-Cu state toward 5s- Sn state. Besides, hybridization will take place between the 3p-S state with 5s or 5p-Sn states and 5s-Sn state with 3d-Cu forming the low of the conduction band.

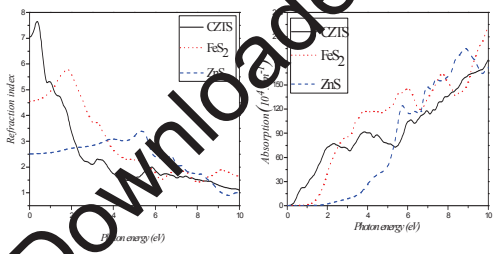

Figure 7. Refractive index and absorption coefficient are calculated as function of photon energy range extended to 10 eV of CZTS, FeS_2 and ZnS materials

4. Conclusion

ZnS material wich replaces efficiently toxic CdS as a buffer layer in CIGS based solar cell is not appropriate for equivalent CZTS structures. A detailed theoretical study of structural, electronic and optical properties of ultra thin films ZnS and FeS2 buffer materials for solar cells has been performed by FP-LAPW method. These results show that FeS2 can be favorably used as buffer in heterostructures with CZTS based solar cells. FeS2 shows interesting physical properties and it is regarded as a promising material for solar cells. On the other hand, the large lattice misfit and the small band offset would cause interface dislocations and reduction of the precipation phase. Furthermore, the variation of chemical environement of films in heterostructure can cause strain and functional hybridation as for example FeS_2 with CZTS absorber.

Acknowledgments

This work was supported by Semiconductor Technology Research Center for Energetic (CRTSE). Some numerical parts were partially helped by Austrian Technik Center, that I would like to thank in particular P. Blaha, K. Schwarz et all for their efforts to develop Wien2k-code.

References

[1] T. K. Todorov, J. Tang, S. Bag, O. Gunawan, T. Gokmen, Y. Zhu and D. B. Mitzi, "Beyond 11% Efficiency: Characteristics of State-of-the-Art $Cu_2ZnSn(S,Se)_4$ Solar Cells", Adva. Mater 2012; **DOI**: 10.1002/aenm.201200348.

[2] A. Nagoya, R. Asahi and G. Kresse, "First-principles study of Cu_2ZnSnS_4 and the related band offsets for photovoltaic applications", J. Phys. Condens. Matter 2011; **23:** 404203.

[3] A. Nagoya, R. Asahi, R. Wahl and G. Kresse, "Defect formation and phase stability of Cu_2ZnSnS_4 photovoltaic material", Phys. Rev. B 2010; **81**: 113202.

[4] S. Chen, X. G. Gong, A. Walsh and S. H. Wei, "Defect physics of the kesterite thin-film solar cell absorber Cu_2ZnSnS_4", Appl. Phys. Lett 2010; **96**: 021902.

[5] S. Chen, J. H. Yang, X. G. Gong, A. Walsh and S. H. Wei, "Intrinsic point defects and complexes in the quaternary kesterite semiconductor Cu_2ZnSnS_4", Phys. Rev. B 2010; **81**: 245204.

[6] K. Wang, O. Gunawan, T. Todorov, B. Shin, S. J. Chey, N. A. Bojarczuk, D. Mitzi and S. Guha, "Thermally evaporated Cu_2ZnSnS_4 solar cells", Appl. Phys. Lett 2010; **97**: 143508.

[7] K. Biswas, S. Lany and A. Zunger, "The electronic consequences of multivalent elements in inorganic solar absorbers: Multivalency of Sn in Cu_2ZnSnS_4", Appl. Phys. Lett 2010; **96:** 201902.

[8] S. Chen, A. Walsh, Y. Luo, J. H. Yang, X. G. Gong and S. H. Wei, "Wurtzite-derived polytypes of kesterite and stannite quaternary chalcogenide semiconductors", Phys. Rev. B 2010; **82**: 195203.

[9] A. Walsh, S. Chen, X. G. Gong and S. H. Wei, "Crystal structure and defect reactions in the kesterite solar cell absorber Cu_2ZnSnS_4 (CZTS): Theoretical insights", AIP. Conf. Proc 2011; **63-64**:1399.

[10] Z. Zhao, C. Ma, Y. Cao, J. Yi, X. He and J. Qiu, "Electronic structure and optical properties of wurtzite-kesterite Cu_2ZnSnS_4", J. Phys. Lett. A 2012; 11: 057.

[11] R. Khenata, A. Bouhemadou, M. Sahnoun, Ali. H. Reshak, H. Baltache and M. Rabah, "Elastic, electronic and optical properties of ZnS, ZnSe and ZnTe under pressure", J. Com. Mat. Sci 2006; **38**: 29-38.

[12] S. Ves, U. Schwarz, N. E. Christensen, K. Syassen and M. Cardona, "Cubic ZnS under pressure: Optical-absorption edge, phase transition, and calculated equation of state", Phys. Rev. B 1990; **42** : 9113-9118.

[13] M. A. Contreras, B. Egaas, K. Ramanathan, J. Hiltner, A. Swartzlander, F. Hasson and R. Noufi: Prog. Photovoltaics **7(4)** (1999) 311.

[14] S. Chen, X. G. Gong and S. H. Wei, "Band-structure anomalies of the chalcopyrite semiconductors $CuGaX_2$ versus $AgGaX_2$(X=S and Se) and their alloys", Phys. Rev. B 2007; **75:** 205209.

[15] S. B. Zhang, S. H. Wei and A. Zunger, "A phenomenological model for systematization and prediction of doping limits in II–VI and I–III–VI_2 compounds", J. Appl. Phys 1998 ; **83** : 3192.

[16] C. N. R. Rao, F. L. Deepak, G. Gundiah and A. Govindaraj, Prog.Solid State Chem. 31 (2003) 5.

[17] K. B. Tang, Y. T. Qian, J. H. Zeng and X. G. Yang, Adv. Mater. 15 (2003) 448.

[18] P. Blaha, K. Schwarz, G. K. H. Madsen, D. Kvasnicka and J. Luitz, *"WIEN2k, An Augmented Plane Wave + Local Orbitals Program for Calculating Crystal Properties",* Techn. Universitat. Wien: Austria; 2001. ISBN 3-9501031-1-2.

[19] J. P. Perdew, S. Burke and M. Ernzerhof, "Restoring the Density-Gradient Expansion for Exchange in Solids and Surfaces", Phys. Rev. Let 2008 ; **100** : 136406.

[20] G. K. H. Madsen and P. Novák, "Charge order in magnetite. An LDA+U study", Euro. Phys. Lett 2005; 69: 777.

[21] Clas. Person, J. Appl. Phys. **107**, (2010) 053710.

[22] M. Gajdos, K. Hummer, G. Kresse, J. Furthmüller and F. Bechstedt, Phys. Rev. B **73** (2006) 045112.

[23] J. Muscat, A. Hung, S. Russo and I. Yarovsky, "First-principles studies of the structural and electronic properties of pyrite FeS_2", Phys. Rev. B 2002 ; **65** : 054107.

[24] R. A. Pollak, L. Ley, S. P. Kowalczyk, D. A. Shirley, J. Joannopoulos, D. J. Chadi and M. L. Cohen, "X-Ray Photoemission Valence-Band Spectra and Theoretical Valence-Band Densities of States for Ge, GaAs, and ZnSe", Phys. Rev. Lett 1972 ; 29 : 1103.

[25] C. F. Klingshirn, "Semiconductor Optics", Springer, Berlin, 1995.

[26] F. D. Murnaghan, Proc Natl Acad Sci USA 1944 ; **30**: 244.

[27] J. P. Leitão, N. M. Santos, P. A. Fernandes, P. M. P. Salomé, A. F. da Cunha, J. C. González and F.M. Matinaga, Thin Solid Films 519 (2011) 7390–7393.

[28] G. S. Babu, Y. B. K. Kumar, P. U. Bhaskar, and V. S. Raja, Semicond. Sci. Technol. **23**, 085023 (2008).

[29] H. Nozaki, T. Fukano, S. Ohta, Y. Seno, H. Katagiri and K. Jimbo, "Crystal structure determination of solar cell materials: Cu_2ZnSnS_4 thin films using X-ray anomalous dispersion", J. Alloys and Compd 2012; 524: 22–25.

[30] V. Kheraj, K. K. Patel, S. J. Patel, D. V. Shah, "Synthesis and characterisation of Copper Zinc Tin Sulphide (CZTS) compound for absorber material in solar-cells", Journal of Crystal Growth 2011; **DOI**:10.1016/j.jcrysgro.2011.10.034.

[31] S. Ves, U. Schwarz, N. E. Christensen, K. Syassen and M. Cardona,"" Phys. Rev. B 1990 ; **42** : 9113.

[32] J. C. Jamieson and H. H. Jr. Demarest., J. Phys. Chem. Solids 1980; **41:** 903.

[33] R. Gangadharan, V. Jayalakshmi, J. Kalaiselvi, S. Mohan, R. Murugan, B. Palanivel, J. Alloy. Compd 2003 ; **5**

[34] R. A. Casali and N. E. Christensen, Solid. State Commun. 108 (1998) 793.

[35] Guanzhou Qiu, Qi. Xiao, Yuehua Li, Wenqing Qin, and Dianzuo Wang, "Theoretical study of the surface energy and electronic structure of pyrite FeS2 (100) using the total-energy pseudopotential method, CASTEP", J. Colloid and Interface Science 270 (2004) 127–132.

[36] D. J. Vaughan, J. R. Craig, "Mineral Chemistry of Metal Sulfide", Cambridge. Univ. Press, London, 1978.

[37] C. Persson and A. Zunger, "$s-d$ coupling in zinc-blende semiconductors", Phys. Rev. B 2003; **68** : 073205.

[38] D. Huang and C. Persson, "Band gap change induced by defect complexes in Cu_2ZnSnS_4", Thin. Solid. Films 2012 ; **DOI** : 10.1016 /j.tsf.2012.10.030.

[39] S. Ahmed, K. B. Reuter, O. Gunawan, L. Guo, L. T. Romankiw and H. A. Deligianni, "High Efficiency Electrodeposited Cu2ZnSnS4 Solar Cell", Adv. Energy. Mater 2012; **2**: 253-259.

[40] D. Aaron, R. Barkhouse, O. Gunawan, T. Gokmen, T. K. Todorov and D. B. Mitzi, "Device characteristics of a 10.1% hydrazine-processed $Cu_2ZnSn(Se,S)_4$ solar cell", Prog. Photovolt: Res Appl 2012; 20: 6-11.

[41] F. Liu, Y. Li, K. Zhang, B. Wang, C. Yan, Y. Lai, Z. Zhang, J. Li, Y. Liu, "In situ growth of Cu_2ZnSnS_4 thin films by reactive magnetron co-sputtering", Sol. Energy. Mater. Sol. Cells 2010 ; **94** : 2431.

[42] M. Jiang, Y. Li, R. Dhakal, P. Thapaliya, M. Mastro, J. D. Caldwell, F. Kub and X. Yan, "Cu_2ZnSnS_4 polycrystalline thin films with large densely packed grains prepared by sol-gel method", J. Photon. Energy 2011; **1**: 019501.

[43] J. P. Perdew and Y. Wang, "Accurate and simple analytic representation of the electron-gas correlation energy", Phys. Rev. B 1992 ; **45** : 13244.

[44] Z. Nourbakhsh, "First principles study of the structural, electronic and optical properties of ZnS_xSe_{1-x} alloys", J. Physica. B 405 (2010) 4173–4187.

[45] A. Yamada, K. Matsubara, K. Sakurai, S. Ishizuka, H. Tampo, P. J. Fons, K. Iwata and S. Niki, Appl ; Phys. Lett (2004) ; **85** : 5607.

[46] V. L. Shaposhnikov, A. V. Krivosheeva, V. E. Borisenko, and J. L. Lazzari, "27th European Photovoltaic Solar Energy Conference and Exhibition", (2012).